Anisotropic Ballistic In-Plane Transport of Electrons in Strained Si

F. M. Bufler[a], S. Keith[b], and B. Meinerzhagen[b]

[a]Institut für Integrierte Systeme, ETH Zürich
CH-8092 Zürich, Switzerland (E-mail: bufler@iis.ee.ethz.ch)
[b]Institut für Theoretische Elektrotechnik und Mikroelektronik
Universität Bremen, D-28334 Bremen, Germany

Abstract

Stationary velocity-field characteristics and transient velocity overshoot along the ⟨100⟩ *and* ⟨110⟩ *field directions are investigated at 300 K with full-band Monte Carlo simulation for electrons in unstrained and (001)-strained Si grown on a* $Si_{0.7}Ge_{0.3}$ *substrate. A pronounced anisotropy of more than 30 % is found for the overshoot peak in strained Si, attaining in the advantageous* ⟨100⟩ *direction a peak value of* 3.4×10^7 *cm/s for a suddenly applied field of 100 kV/cm. The energy relaxation time, necessary for hydrodynamic device simulation of the overshoot effect, changes from 0.3 ps in unstrained Si to 0.4 ps in strained Si.*

1. Introduction

MOSFETs based on strained Si/SiGe structures are currently regarded as devices which may take us to the outermost limits of silicon scaling [1]. Device operation in this nanometer regime is characterized by high-field and ballistic effects, which are strongly influenced by the band structure. The well-known differences of the curvatures between the ⟨100⟩ and ⟨110⟩ directions in the warped hole bands of unstrained Si have recently been shown to have a decisive influence on ballistic transport [2]. This situation is much less obvious for the ellipsoidal conduction band valleys in unstrained and strained Si, and work on non-linear electron transport in strained Si has not yet addressed this important issue [3, 4, 5, 6]. Therefore, full-band Monte Carlo simulation is employed in this paper to investigate the anisotropy of high-field and transient overshoot effects for electrons in unstrained and strained Si.

2. Model

The full bandstructures were computed using the non-local empirical pseudopotential method [7] where, in addition, the spin-orbit interaction in Si has also been taken into account. The phonon scattering mechanisms comprise acoustic intravalley phonons in the elastic equipartition approximation as well as f-type and g-type intervalley processes according to Jacoboni and Reggiani [8]. The only modification consists of a multiplication of the coupling constants by a global factor of 0.97. This Monte

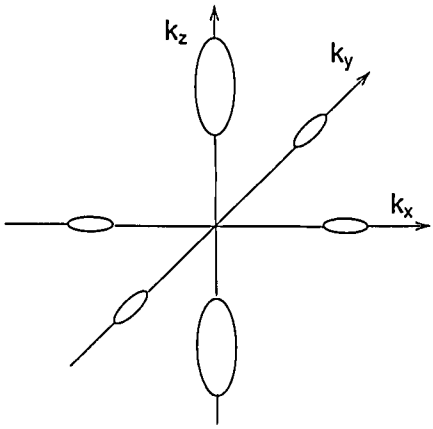

Figure 1: Equienergetic surfaces of the first conduction band in Si under biaxial tensile strain. The z direction corresponds to the growth direction.

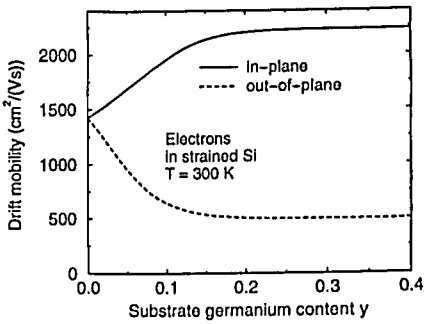

Figure 2: Ohmic in-plane and out-of-plane drift mobility at 300 K for electrons in a strained Si layer grown on an (001) $Si_{1-y}Ge_y$ substrate

Carlo model has been verified by comparison with experimental transport data over a wide range of lattice temperatures and electric field strengths [9]. Under biaxial tensile strain caused by growing a Si layer along the (001) direction on a $Si_{1-y}Ge_y$ substrate four of the six conduction band valleys are shifted upwards in energy. This is illustrated in Fig. 1 by the equienergy surfaces of strained Si in the low-energy region. The small transverse mass and the large longitudinal mass experienced by the electrons in the two lower valleys in direction parallel ("in-plane") and perpendicular ("out-of-plane") to the Si/SiGe interface, respectively, explains the increase and decrease of the corresponding Ohmic drift mobility components shown in Fig. 2.

3. Results

The results for non-linear in-plane transport along the ⟨100⟩ and ⟨110⟩ crystallographic directions under stationary and transient conditions, respectively, are depicted in Figs. 3 and 4. In unstrained Si, the stationary drift velocity for a field applied in the ⟨110⟩ direction is always larger than for a ⟨100⟩ field direction, while the opposite behavior can be seen for the corresponding transient velocity overshoot peaks. This situation can still be qualitatively understood within the standard analytic anisotropic electron band model [8]. For a field along the ⟨100⟩ direction, transport of electrons in four of the six valleys is characterized by the small transverse mass, and the ballistic overshoot is consequently larger than for the ⟨110⟩ direction. The high energy gained by the electrons in these four valleys enhances in turn intervalley scattering, which finally leads to a preferred population of the two valleys with the large longitudinal mass and therefore to a smaller stationary drift velocity [10]. However, the analytic band model predicts in strained Si, where almost all electrons are in the two lower valleys, also in the non-linear and ballistic regime exactly the same drift velocities for the ⟨100⟩ and ⟨110⟩ directions. This is in contrast to strongly different full-band results for those two cases, where Figs. 3 and 4 show larger drift velocities in the ⟨100⟩ direction for the stationary and especially for the overshoot velocity. The reason is that the curvatures of the energy in a conduction band valley

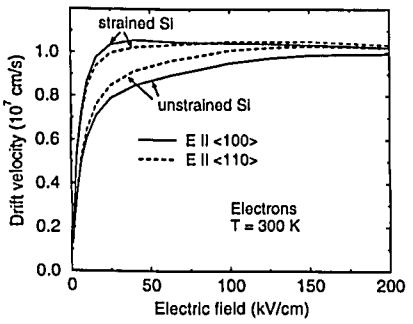

Figure 3: In-plane velocity–field characteristics with the field parallel to ⟨100⟩ and ⟨110⟩ directions, respectively, of electrons at 300 K in unstrained Si and in strained Si grown on a $Si_{0.7}Ge_{0.3}$ substrate

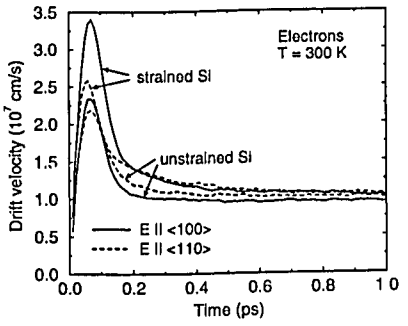

Figure 4: Transient in-plane velocity overshoot with a sudden application of a 100 kV/cm field for the same configurations as in Fig. 3

start to differ drastically above 100 meV between the ⟨100⟩ and the ⟨110⟩ direction while being exactly the same in the standard analytic band model. This is shown by the energy dispersion relation for strained Si in Fig. 5. A similar situation can be found for unstrained Si, but the consequences do not show up due to valley repopulations as explained above. However, the limiting case of unstrained Si is also recovered in strained Si at the highest field strengths in Fig. 3. In this high-field regime the four energetically higher valleys in strained Si are populated as well and the stationary drift velocity in ⟨110⟩ direction becomes larger than in ⟨100⟩ direction as it is the case for unstrained Si. Finally, we report in Fig. 6 the energy relaxation times in unstrained and strained Si as a function of the equivalent electron temperature which is proportional to the mean energy. The energy relaxation times are necessary for hydrodynamic device simulation and turn out to change roughly from 0.3 ps in unstrained Si to 0.4 ps in strained Si grown on a $Si_{0.7}Ge_{0.3}$ substrate. On the other hand, they can be seen to be in both cases insensitive to the field direction. For unstrained Si this points to a principal limitation of the hydrodynamic model in describing accurately ballistic overshoot effects, because the same energy relaxation times in both field directions in conjunction with a larger stationary drift velocity in ⟨110⟩ direction cannot lead to a smaller overshoot in this field direction. This effect is, however, of minor importance for practical applications due to the small differences of the overshoot peaks in unstrained Si.

4. Conclusions

We have shown by full-band Monte Carlo simulation that transient ballistic in-plane overshoot of electrons in strained Si is significantly larger in the ⟨100⟩ direction than in ⟨110⟩ direction. In addition, we have demonstrated the failure of Monte Carlo models based on analytic electron band structures in describing the anisotropy of ballistic in-plane transport in strained Si as well as the limits of hydrodynamic models in reproducing anisotropic ballistic overshoots effects in unstrained Si.

Acknowledgments We would like to thank M. M. Rieger for calculating the band structures and P. Graf for useful discussions. This work was supported in part by the Bundesministerium für Bildung, Wissenschaft, Forschung und Technologie.

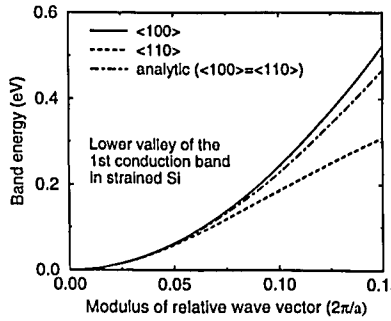

Figure 5: Electron energy in a lower valley of strained Si vs. modulus of the wave vector (measured with respect to the valley minimum) along two directions perpendicular to the k_z axis in Fig. 1

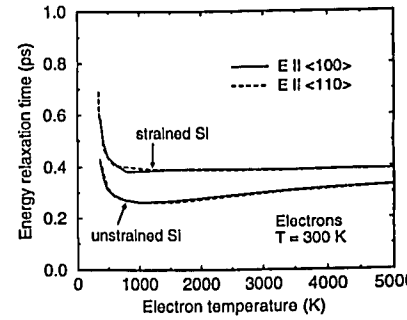

Figure 6: Energy relaxation times as a function of the electron temperature for the configurations shown in Figs. 3 and 4

References

[1] Y. Taur, D. A. Buchanan, W. Chen, D. J. Frank, K. E. Ismail, S.-H. Lo, G. A. Sai-Halasz, R. G. Viswanathan, H.-J. C. Wann, S. J. Wind, and H.-S. Wong, "CMOS scaling into the nanometer regime," *Proc. IEEE*, vol. 85, pp. 486–504, 1997.

[2] Y. Tagawa, Y. Awano, and N. Yokoyama, "Anisotropic hole velocity overshoot in GaAs and Si," in *HCIS Abstracts*, p. ThP34, 1997.

[3] H. Miyata, T. Yamada, and D. K. Ferry, "Electron transport properties of a strained Si layer on a relaxed $Si_{1-x}Ge_x$ substrate by Monte Carlo simulation," *Appl. Phys. Lett.*, vol. 62, pp. 2661–2663, 1993.

[4] T. Vogelsang and R. K. Hofmann, "Electron transport in strained si layers on $Si_{1-x}Ge_x$ substrates," *Appl. Phys. Lett.*, vol. 63, pp. 186–188, 1993.

[5] F. M. Bufler, P. Graf, S. Keith, and B. Meinerzhagen, "Full band Monte Carlo investigation of electron transport in strained Si grown on $Si_{1-x}Ge_x$ substrates," *Appl. Phys. Lett.*, vol. 70, pp. 2144–2146, 1997.

[6] S. Keith, F. M. Bufler, and B. Meinerzhagen, "Full band Monte-Carlo device simulation of an 0.1 μm n-channel MOSFET in strained silicon material," in *Proc. ESSDERC*, vol. 27, pp. 200–203, 1997.

[7] M. M. Rieger and P. Vogl, "Electronic-band parameters in strained $Si_{1-x}Ge_x$ alloys on $Si_{1-y}Ge_y$ substrates," *Phys. Rev. B*, vol. 48, pp. 14276–14287, 1993.

[8] C. Jacoboni and L. Reggiani, "The Monte Carlo method for the solution of charge transport in semiconductors with application to covalent materials," *Rev. Mod. Phys.*, vol. 55, pp. 645–705, 1983.

[9] F. M. Bufler, *Full-Band Monte Carlo Simulation of Electrons and Holes in strained Si and SiGe*. Munich: Herbert Utz Verlag, 1998 (http://utzverlag.com).

[10] C. Canali, G. Ottaviani, and A. Alberigi-Quaranta, "Drift velocity of electrons and holes and associated anisotropic effects in silicon," *J. Phys. Chem. Solids*, vol. 32, pp. 1707–1720, 1971.